Received: 22 January 2018 | Revised: 6 August 2018 | Accepted: 7 September 2018

DOI: 10.1002/env.2540

Check for updates

SPECIAL ISSUE PAPER

WILEY

A study of links between the Arctic and the midlatitude jet stream using Granger and Pearl causality

S. M. Samarasinghe[1] | M. C. McGraw[2] | E. A. Barnes[2] | I. Ebert-Uphoff[1]

[1]Department of Electrical and Computer Engineering, Colorado State University, Fort Collins, Colorado

[2]Department of Atmospheric Science, Colorado State University, Fort Collins, Colorado

Correspondence
I. Ebert-Uphoff, Department of Electrical and Computer Engineering, Colorado State University, Fort Collins, CO 80523.
Email: iebert@colostate.edu

Funding information
National Science Foundation, Grant/Award Number: AGS-1545675 (Barnes and McGraw) and AGS-1445978 (Ebert-Uphoff and Samarasinghe)

Abstract

This paper investigates causal links between Arctic temperatures and the jet streams. We apply two different frameworks for this application based on the concepts of (1) *Granger causality* and (2) *Pearl causality*. Both methods show that Arctic temperature and jet speed and position all exhibit strong autocorrelation, but they also show that these variables are linked together by two robust positive feedback loops that operate on time scales of 5–25 days. The dynamical implications of these feedbacks are discussed. This study is only the beginning of a larger effort to apply and compare different causality methods in order to gain a deeper understanding of the causal connections between the Arctic and weather at lower latitudes.

KEYWORDS

Arctic, causality, feedback, jet stream, regression, structure learning

1 | MOTIVATION

Arctic amplification, that is, the phenomenon of Arctic temperatures rising much faster than the global mean (Serreze & Barry, 2005), and its present and future effects on midlatitude weather and climate have received substantial attention in recent years. While it is well known that the midlatitude circulation can drive changes in Arctic temperatures and sea ice, it is unclear how and to what extent the Arctic influences midlatitude weather (Barnes & Screen, 2015). Some argue that Arctic amplification is already influencing midlatitude weather (Francis & Vavrus, 2012; Liu, Curry, Wang, Song, & Horton, 2012; Overland & Wang, 2010; Tang, Zhang, Yang, & Francis, 2013), whereas others state that any possible signal is too small to have been observed amidst the background of atmospheric variability (Barnes, 2013; Barnes, Dunn-Sigouin, Masato, & Woollings, 2014; Screen & Simmonds, 2010). Regarding Arctic influence on the midlatitude circulation under climate change, idealized and fully coupled climate model simulations have shown an equatorward shift of the jet streams and storm tracks (the regions where extratropical cyclones occur most frequently) as well as weakening of the zonal winds in response to Arctic warming and sea ice loss (Butler, Thompson, & Heikes, 2010; Deser, Tomas, Alexander, & Lawrence, 2010; Magnusdottir, Deser, & Saravanan, 2004; Peings & Magnusdottir, 2014). The mean locations of the wintertime jet streams in MERRA-2 reanalysis data (Gelaro et al., 2017) can be seen in Figure 1a. While this equatorward shift of the storm tracks is considered a robust midlatitude response to Arctic amplification, little is understood about the underlying dynamics behind this response in models or whether the models can adequately simulate the processes involved. Making progress requires that we study the two-way causal connections between Arctic temperatures and the midlatitude circulation, that is, the midlatitude circulation driving changes in the Arctic and the Arctic driving changes in the midlatitudes, in context of one another and the background of atmospheric variability.

The typical approach for assessing causal links in climate dynamics (including studying the links between the jet streams and Arctic warming/sea ice loss) is targeted modeling studies. While incredibly useful for understanding the

 © 2018 John Wiley & Sons, Ltd.

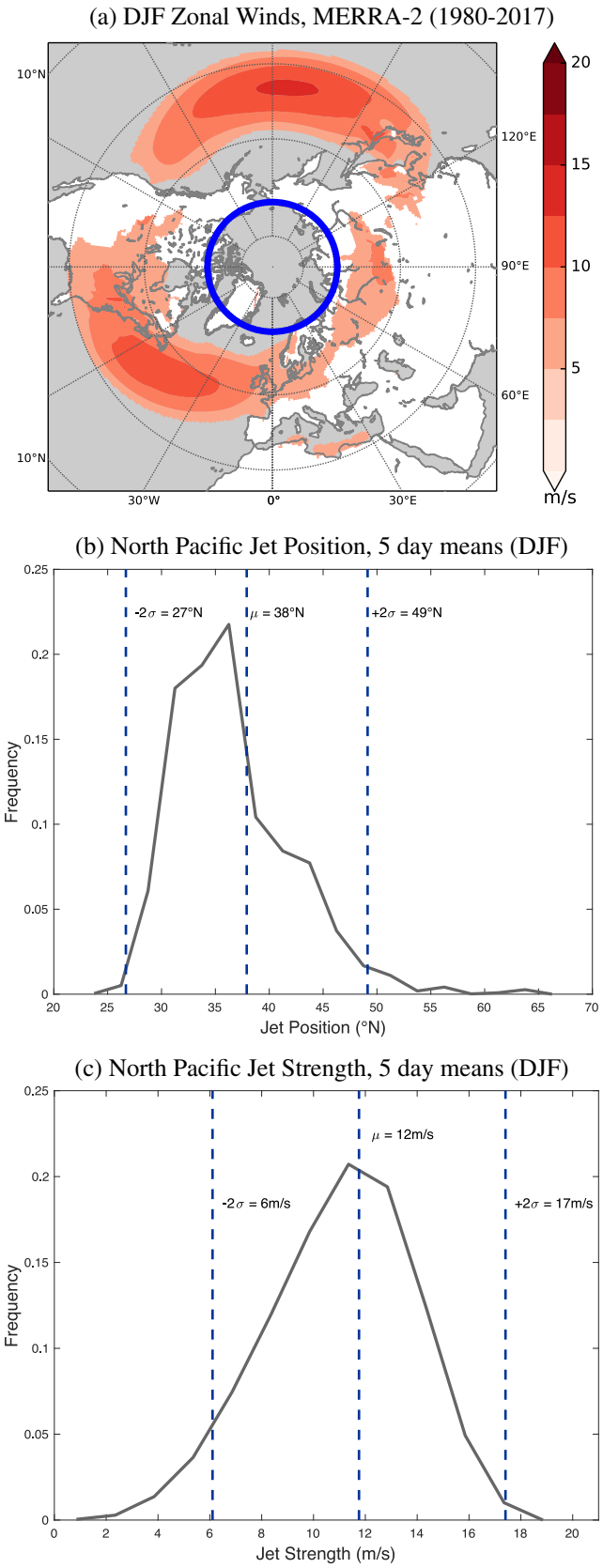

FIGURE 1 (a) Daily mean December–January–February (DJF) zonal winds calculated from MERRA-2 reanalysis. Only values above 5 m/s are shown. The blue line denotes 70°N and indicates the cap over which $\mathcal{T}$ is calculated. Distributions of DJF North Pacific jet (b) position and (c) strength. Dashed lines indicate mean (μ) and two standard deviations ($\pm 2\sigma$)

physical mechanisms at play, this approach only allows for studying cause and effect in isolation and does not allow for the feedbacks between the jet streams and Arctic warming to fully develop. A modeling study that examines the response of the atmospheric circulation to prescribed heating in the Arctic analyzes the circulation response to this Arctic warming; however, as the heating in the Arctic is fixed, the circulation is unable to influence, modify, or feed back upon the Arctic temperature. However, the midlatitude circulation is thought to have substantial impacts on the Arctic, potentially impacting Arctic temperatures, sea ice thickness and extent, and moisture (Liu & Barnes, 2015; Overland & Wang, 2010; Woods, Caballero, & Svensson, 2013). These two-way feedbacks are potentially very important in terms of understanding the full atmospheric response to Arctic warming, and thus, it is vital to analyze both the Arctic's influence on the midlatitudes and vice versa.

In addition, we have entered a period where atmospheric science tends to be "data rich" both in observations and model output (Overpeck, Meehl, Bony, & Easterling, 2011). Thus, there is great need for additional tools that can aid scientists in identifying and extracting signals. Causal discovery techniques (1) provide robust definitions of causality, (2) can have direct ties to forecasting/prediction, (3) augment targeted model studies, and (4) allow for a direct comparison of results from observations and models.

Here, we use two different frameworks to learn about causal relationships for the Arctic-midlatitude system. The first framework uses vector autoregression (VAR)-type models (i.e., VAR and least absolute shrinkage and selection operator [LASSO]), combined with the concept of *Granger causality*. The second framework is based on the concept of *Pearl causality*. We apply both frameworks to the study of causal links between the Arctic and midlatitude jet streams. The purpose is two-fold: By comparing the results of two very different frameworks, we hope (1) to identify robust results and (2) to make more geoscientists aware of the different types of causal analysis tools. In this journal article, we extend and progress from our initial study presented as a short paper (Samarasinghe, McGraw, Barnes, & Ebert-Uphoff, 2017), while providing detailed elaborations.

2 | CAUSALITY IN CLIMATE SCIENCE

The best known concept to identify cause–effect relationships in climate science is *Granger causality*, developed by Clive Granger in the late 1960s (Granger, 1969, 1980); see Section 4.1.1. However, other methods for causal discovery also exist, including *Pearl causality*, which was developed in the late 1980s (Pearl, 1988, 2000; Rebane & Pearl, 1987; Spirtes, Glymour, & Scheines, 2000); see Section 4.2. When investigating cause–effect relationships, it is crucial to distinguish between two different types of causal analysis, namely, (1) intervention analysis and (2) observational analysis. *Causal calculus* (Pearl, 1988; Rebane & Pearl, 1987), which provides a comprehensive mathematical framework for causal discovery, analyzes what can or cannot be concluded using either type of analysis. Intervention analysis allows one to positively prove or disprove causal relationships between considered variables, but it requires that scientists can actually perform interventions on the system of study, that is, that one can *change* the state of any variable and then observe the cascading effects on the other variables. In climate science, such interventions are very difficult and most often require the use of dynamical models and a specific experimental design (Hannart, Pearl, Otto, Naveau, & Ghil, 2016).

Here, instead of performing multiple dynamical model simulations to act as interventions, we focus solely on an observational-type analysis, using model output that already exists in place of actual observations. Several different frameworks for observational analysis have been applied to climate science to provide graphical representations of likely cause–effect relationships (Bahadori & Liu, 2011; Chen, Liu, Liu, & Carbonell, 2010; Chu, Danks, & Glymour, 2005; Ebert-Uphoff & Deng, 2012; Ebert-Uphoff & Deng, 2015; McGraw & Barnes, 2018; Runge, 2014; Runge, Heitzig, Petoukhov, & Kurths, 2012; Wang, Banerjee, Hsieh, Ravikumar, & Dhillon, 2013; Zerenner, Friederichs, Lehnertz, & Hense, 2014). However, of highest relevance to the application considered here are causality studies related to the Arctic, primarily the works by Strong, Magnusdottir, and Stern (2009), Matthewman and Magnusdottir (2011), and Kretschmer, Coumou, Donges, and Runge (2016). These studies demonstrate the utility of causality techniques for studying Arctic-midlatitude connections. Strong et al. (2009) and Matthewman and Magnusdottir (2011) use a VAR-Granger approach to explore sea ice-North Atlantic oscillation and sea ice-West Pacific pattern connections, respectively. Their approach falls into the category of Granger approaches discussed in Section 4.1.1. While Strong et al. (2009) and Matthewman and Magnusdottir (2011) assess the performance and significance of their VAR model and its results by comparing an unrestricted model (all connections are allowed) to a restricted model (specific connections are not permitted), here we assess significance by comparing an unrestricted VAR-Granger model (similar to that described in

Strong et al., 2009) to a LASSO model that uses regularized regression to determine significant coefficients and connections (see Section 4.1.4). Another difference between our work and that of Strong et al. (2009) and Matthewman and Magnusdottir (2011) is that these previous studies allow for simultaneous connections, whereas we, for simplicity, do not.

Kretschmer et al. (2016) use a combination of Pearl causality and Granger causality concepts to investigate the role of Barents–Kara Sea ice concentrations on wintertime circulation using a two-step procedure. In Step 1, they identify, for each considered variable, its potential causes using Pearl causality. Step 2 uses Granger causality, namely, they perform a regression analysis for each variable to verify the results obtained in Step 1 and to assess the strength of the connections. Both steps are performed separately for each variable, that is, one variable is declared the output variable (predictand) and the effect of all other variables (predictors) on the specific output variable is studied using scalar regression models. The results from these individual analyses are then pieced together at the end to a combined graph of all interactions. In contrast, we promote using a vector approach that studies relationships between all variables simultaneously, without declaring any of them predictand or predictor, which allows for feedback loops between the variables to be explicitly identified. Nevertheless, the method by Kretschmer et al. (2016) is most closely related to the work presented here.

Another difference between our work and previous studies (e.g., Kretschmer et al., 2016; Matthewman & Magnusdottir, 2011; Strong et al., 2009) is that previous studies use empirical orthogonal functions to represent the circulation response to Arctic warming. While empirical orthogonal function-based methods can be quite useful at dimension reduction and capturing broad-scale spatial variability, they often fail to capture details in the circulation changes. By focusing here on the position and strength of the jet streams separately, we are able to analyze potential circulation changes in more detail, as jet position and jet strength do not necessarily covary (Thomas, Waugh, & Gnanadesikan, 2015; Woollings et al., 2018).

3 | DATA

We analyze daily data from the Community Earth System Model Large Ensemble (CESM-LE; Kay et al., 2015), a fully coupled general circulation model. We use years 402 to 2,200 of the preindustrial control run (all external forcing is fixed at its levels from 1850), resulting in 656,634 days (1,798 years) of data that acts as a proxy for a very long observational record. The data are gridded at a 1° horizontal grid spacing, that is, 0.9° in latitude by 1.25° in longitude. The seasonal cycle is removed from the daily data, and the daily data are then averaged into nonoverlapping 5-day chunks to smooth out higher frequency variability. Afterwards, each time series is standardized, that is, its mean is subtracted and it is divided by its standard deviation. For our analysis, we focus on the winter season December, January, and February (DJF), roughly dividing the number of data samples for each experiment by four.

The data are stationary in the long term, as they were generated by a control run with no external forcing, and the impacts of the seasonal cycle are minimized by removing the first four Fourier harmonics of the data. Nevertheless, as pointed out by Lund, Hurd, Bloomfield, and Smith (1995), even if the seasonal cycle is removed in this way, there is still the possibility that seasons affect the relationship between the different variables, which would necessitate taking the cycle into account when modeling their causal relationships. This is not a concern in this study, as we only consider a single season (December–February), and any seasonal changes can be assumed to be sufficiently small during that time. (Otherwise, one could use the tools provided in Lund et al., 1995, to test for periodic correlation and to adjust the model accordingly.) The mean subtraction in the standardization ensures that all variables used in the models have zero means. However, this step has minimal impact on the results as the variables already have means that are almost zero (but not exactly zero) at this stage. The winter season is analyzed here because the teleconnection patterns between different regions are strongest in winter (Wallace & Gutzler, 1981), and extratropical storm activity itself is greatest in winter (Hoskins & Hodges, 2002; Wettstein & Wallace, 2010). Here, we focus on the North Pacific (120° E–240° E, covering 97 grid boxes in longitude), and we analyze the circulation using the following three univariate time series, each consisting of 32,381 5-day averages:

- jet latitude in the North Pacific, $\mathcal{L}$;
- jet speed in the North Pacific, $\mathcal{S}$; and
- 850 hPa Arctic temperature averaged over 70° N–90° N at all longitudes, $\mathcal{T}$.

Jet latitude, $\mathcal{L}$, and jet speed, $\mathcal{S}$, represent the position and strength of the eddy-driven jet, which are often used as proxies for the position and strength of the jet streams. $\mathcal{L}$ and $\mathcal{S}$ are calculated by determining the maximum position and strength of the zonal component of the winds at 850 hPa over the North Pacific basin (120° E–240° E). First, the 850 hPa zonal winds are averaged over all longitudes in the North Pacific basin to create a zonal-mean profile of the zonal wind. The resulting zonal-mean zonal wind profile is interpolated to a 0.01° latitude grid. A quadratic polynomial is fit around the maximum of this interpolated wind profile, following the work of Woollings, Hannachi, and Hoskins (2010); see figure S3 in the work of Barnes and Fiore (2013) for an example of a zonal-mean zonal-wind profile. The maximum of this quadratic polynomial is the jet speed ($\mathcal{S}$), whereas its latitudinal position is the jet latitude ($\mathcal{L}$). The distributions of 5-day mean wintertime North Pacific jet position (Figure 1b) and jet strength (Figure 1c) can be seen in Figure 1, with their means and spreads indicated by vertical lines. Note that the seasonal cycle has not been subtracted from the jet position and jet speed distributions in Figure 1b,c, so as to show the actual physical values of North Pacific wintertime jet position and speed.

4 | CAUSALITY METHODS

We briefly discuss the two types of causality methods used here, based on (1) Granger causality and (2) Pearl causality.

4.1 | Methods based on Granger causality

In this subsection, we discuss the concept of Granger causality and introduce two types of regression models, VAR models and LASSO models, which can be used to identify variables that are *Granger causes* of other variables.

4.1.1 | Granger causality

The concept of Granger causality is based on the predictability of temporal variables and can be simply explained using two univariate time series $X = \{x_t\}_{t=1}^{T}$ and $Y = \{y_t\}_{t=1}^{T}$. The time series X is said to be a *Granger cause* of Y, if the past values of X provide information about the current state of Y, beyond what is already known from the past values of Y, alone. Testing for Granger causality can thus be achieved by comparing two different prediction models. In the first model, Y is predicted using the past values of both X and Y (unrestricted model), whereas in the second model, Y is predicted using only the past values of Y (restricted model). Then, a statistical test is carried out to determine whether the unrestricted model significantly improves the predictability of Y compared to the restricted model; for details, see for example the work of Strong et al. (2009). If the predictability of Y is significantly improved by the inclusion of X in the model, X is said to Granger cause Y. As for the prediction model, a suitable linear or nonlinear model can be used. In the context of this paper, we only look at linear lagged regression models resulting in restricted and unrestricted models as follows:

$$\text{Unrestricted model:} \quad y_t = \beta + a_1 y_{t-1} + a_2 y_{t-2} + \ \dots \ + a_s y_{t-s} + c_1 x_{t-1} + c_2 x_{t-2} + \ \dots \ + c_p x_{t-p} \tag{1}$$

$$\text{Restricted model:} \quad y_t = \gamma + b_1 y_{t-1} + b_2 y_{t-2} + \ \dots \ + b_s y_{t-s}. \tag{2}$$

Here, a_i, b_i (for integer $i \in [1, s]$) and c_j (for integer $j \in [1, p]$) are scalar regression coefficients and β and γ are model intercepts. p and s are the number of lags of X and Y, respectively. For simplicity, we use the same number of lags for each variable, that is, $s = p$.

This approach, which we call the *two-model Granger* approach, is the simplest and by far the most common approach in which Granger causality is used in climate science to date. The use of Granger causality in this way constitutes a major step forward compared with more traditional methods in climate science such as single-variable lagged linear regression analysis because the latter can often lead to misleading conclusions, which are prevented with the two-model Granger approach (McGraw & Barnes, 2018). The two-model Granger approach can be extended by connecting the concept of Granger causality to the coefficients of VAR models. This approach, which we call *VAR-Granger*, is a natural generalization of the two-model Granger approach, which allows us to (1) easily apply Granger analysis in cases with a large number of

time series variables and (2) generate visualizations of the different relationships in the form of graphs, as demonstrated in later sections.

4.1.2 | VAR model

VAR performs regression on several variables *without* declaring one variable the predictand and the remaining ones the predictors. Instead, all variables are treated the same way. Namely, a VAR(p) model estimates the vector $\mathbf{z}_t \in \mathbb{R}^k$, which contains *all* variables of interest, in terms of its p lags as follows:

$$\mathbf{z}_t = \mathbf{c} + \mathbf{A}_1\mathbf{z}_{t-1} + \ \dots\ + \mathbf{A}_p\mathbf{z}_{t-p} + \mathbf{e}_t \quad \text{for} \quad t = (p+1),\ \dots, T, \tag{3}$$

where vector $\mathbf{z}_t = [z_{1t},\ \dots\ , z_{kt}]'$ contains the values of k considered variables at time t; $\mathbf{c} = [c_1,\ \dots\ , c_k]'$ is a fixed vector containing the model intercepts; $\mathbf{A}_i$ are the $(k \times k)$ coefficient matrices (for $i = 1,\ \dots\ , p$); and $\mathbf{e}_t = [e_{1t},\ \dots\ , e_{kt}]'$ is the vector of error terms (residuals). These error terms are assumed to be independent and identically distributed with $E[\mathbf{e}_t] = 0$ and a nonsingular covariance matrix $E[\mathbf{e}_t\mathbf{e}_t'] = \Sigma_e$. Using this notation, to analyze the relationships between the two univariate time series X and Y from Section 4.1.1, we would simply use $k = 2$ and define $\mathbf{z}_t = [x_t, y_t]'$.

An ordinary least-squares approach is used to solve the standard regression problem and calculate the model parameters of Equation (3), namely, vector $\mathbf{c}$ and matrices $\mathbf{A}_i$ (Lütkepohl, 2007). Once a model of the form in Equation (3) is obtained, we perform a validation test to ensure that the model is stable, that is, that all roots of the characteristic polynomial lie outside the complex unit circle (e.g., see Lütkepohl, 2007; Pfaff, 2008). Such a stable VAR(p) process is automatically stationary as well. We derive such a VAR model for several different values of p and select a suitable model using a selection criterion, such as the Akaike information criterion or the Bayesian information criterion (Ivanov & Kilian, 2005; Lütkepohl, 2007; Nicholson, Matteson, & Bien, 2017).

4.1.3 | Connection to Granger causality

We can apply the concept of Granger causality to VAR models by inspecting the coefficients in $\mathbf{A}_i$. Let a^i_{lm} denote the element of row l and column m of matrix $\mathbf{A}_i$, and let the time series $\{z_{l,t}\}$ denote the lth variable without lag and $\{z_{m,t-i}\}$ denote the mth variable with lag i. Then, a^i_{lm} denotes the effect of $\{z_{m,t-i}\}$ on $\{z_{l,t}\}$. Furthermore, because the data was normalized, a^i_{lm} indicates for a change of one standard deviation of $\{z_{m,t-i}\}$ the amount of change to expect in $\{z_{l,t}\}$. (This quantitative interpretation should be used with caution, as many geophysical relationships are nonlinear, and the model is thus only a rough approximation.) Then, for $l \neq m$, we see in this model that $\{z_{m,t-i}\}$ is useful for the prediction of $\{z_{l,t}\}$, if and only if $a^i_{lm} \neq 0$. Consequently, the mth variable, $\{z_m\}$, is said to *Granger cause* the lth variable, $\{z_l\}$, if and only if at least one of the coefficients $a^i_{lm} \neq 0$ for any lag $i = 1,\ \dots\ , p$.

For practical implementation, determining nonzero coefficients from a VAR model often requires applying a threshold on the magnitudes of the coefficients. That is because, due to noise and numerical accuracy, many—sometimes even most—of the coefficients can be very close to zero, but not exactly zero. Unless a natural threshold can be identified based on the problem, we need to set a user-defined threshold, resulting in subjective model selection, which can be highly sensitive to noise. The following section describes how regularized regression techniques can be used to overcome this issue.

4.1.4 | Regularized regression (LASSO)

Regularization techniques can be used to obtain a sparse model that identifies the subset of predictors that have the strongest effect on the predictability of the responses. Specifically, the LASSO (Hastie, Tibshirani, & Wainwright, 2015; Nicholson et al., 2017; Tibshirani, 1996) approach finds a least squares solution subject to an l_1-norm constraint on the coefficients, namely, it imposes a bound on the sum of the absolute values of the coefficients. The imposed constraint shrinks the values of the regression coefficients and sets many coefficients exactly to zero to obtain a more generalized and sparse solution.[1] Therefore, LASSO results in a model of the exact same form as Equation (3), but where many coefficients are exactly zero. This improves the interpretability of the model (especially when there is a large number of predictors)

[1]Note that applying an l_2-norm constraint to the coefficients would also shrink them, but would not force them to zero (Hastie et al., 2015).

and simplifies the process of identifying Granger causes. In addition, regularization allows for a more generalized model with improved prediction accuracy on test data compared to the ordinary least squares solution (Tibshirani, 1996). For this particular study, we use a version of the group LASSO approach, described in the Appendix .

For LASSO approaches, the regularization parameter, λ, determines the sparsity of the resulting matrix. Using $\lambda = 0$ is equivalent to the ordinary least squares solution, whereas a large value of λ gives a very sparse solution. (See Equation (A1) in the Appendix for the exact definition of λ for the group Lasso approach.) λ should be selected as a trade-off, that is, small enough such that all relevant relationships in the model are included, but large enough to yield a simple and interpretable model.

4.2 | Method based on Pearl causality

Pearl causality (Pearl, 1988, 2000; Spirtes et al., 2000) follows from causal calculus (Rebane & Pearl, 1987) and is defined through interventions. If interventions are possible, then Pearl causality provides both *sufficient* and *necessary* conditions for causal relationships, that is, with an intervention analysis, one can say with *certainty* whether or not variable X is a cause of Y. In the case of observational analysis, we can still use Pearl causality to provide a *necessary* condition for causality, namely, certain conditions have to be satisfied in order for X to possibly be a cause of Y. The primary reason for losing the ability to prove sufficiency from observations alone is the potential existence of hidden common causes, that is, *latent confounding variables*. Namely, if two variables X and Y are both related solely due to the effect on them by an unmeasured third variable, Z, then an intervention analysis would correctly identify that there is no direct connection between X and Y, whereas an observational analysis might incorrectly conclude in that case that X is a cause of Y, or vice versa.

In an observational analysis, we can nevertheless use the necessary condition to eliminate the great majority of potential connections, leaving only a small number of potential cause–effect relationships. Namely, we use an elimination method that first assumes that all pairs of variables have cause–effect connections to each other (for all lags), and then uses conditional independence tests as necessary causality conditions to *delete* connections. The best known algorithm for this purpose is the classic *PC* algorithm (Spirtes & Glymour, 1991), which is named after the first names of the two authors, *Peter* Spirtes and *Clark* Glymour. The PC algorithm usually yields a small set of *potential* cause–effect relationships, and the set of *true* causal relationships is a subset of that set.

This type of method is called *constraint-based structure learning*, because we seek to constrain, that is, construct a boundary set for, the set of true causal relationships. The specific method used here is the temporal version (Chu et al., 2005; Ebert-Uphoff & Deng, 2012) of the *PC stable* algorithm (Colombo & Maathuis, 2014). The *PC stable* algorithm is a variant of PC that is more robust and can easily be parallelized. For more details on this approach, see the work of Ebert-Uphoff and Deng (2012). For brevity, we refer to the *PC stable* algorithm as simply PC in the remainder of this document.

5 | APPLICATION TO ARCTIC–JET STREAM CONNECTIONS

To study the causal links between the Arctic and the midlatitude jet streams, we model the relationships between jet speed ($\mathcal{S}$) and Arctic temperature ($\mathcal{T}$), and separately, the relationships between jet latitude ($\mathcal{L}$) and Arctic temperature ($\mathcal{T}$), using the three methods discussed above, that is, the VAR-Granger, LASSO-Granger, and *PC stable* methods.

5.1 | Implementation details

Multivariate regression in VAR is implemented using the *mvregress* function in MATLAB, whereas the *Glmnet* (Qian, Hastie, Friedman, Tibshirani, & Simon, 2013) MATLAB package (multiresponse Gaussian family scenario) is used to apply LASSO. We use the Akaike information criterion and the Bayesian information criterion to select the maximum lag, p, for the VAR model. Here we determine that $p = 5$ (25 days). The λ parameter in LASSO is selected using a K-fold cross validation scheme (with $K = 10$) based on the mean square error performance on test data. Namely, the selected λ

is the λ that corresponds to the *one-standard-error rule*, as explained in the works of Hastie et al. (2015) and Melkumova and Shatskikh (2017); this λ gives a more regularized model, while keeping the mean squared error (MSE) within one standard error of the minimum MSE value. Based on this scheme, $\lambda = 0.0179$ is selected for the $\mathcal{T}$ versus $\mathcal{S}$ model. (Additional information related to the selection of p and λ parameters is provided in the Supporting Material).

The *learn_struct_pdag_pc* function of the MATLAB Bayes Net Toolbox (Murphy, 2014) is used for a simple implementation of the *PC stable* algorithm. We modify the Bayes Net Toolbox to use temporal constraints (Chu et al., 2005; Ebert-Uphoff & Deng, 2012) and implement the *PC stable* version. We use the Fisher-Z test to test for conditional independence using partial correlation. The significance value, α, of the independence test is chosen as $\alpha = 0.05$, a common value; results are insensitive to variations in α between 0.01 and 0.1. Instantaneous connections are not permitted between variables in the *PC stable* algorithm to make results comparable with VAR and LASSO implementations. The PC model is run with 11 time slices using the original variables $\{z\}$ and 10 time shifted versions of $\{z\}$ shifted by $-25, -20, \ldots, -5, +5, \ldots, +25$ days (Ebert-Uphoff & Deng, 2012). As general practice, we check convergence characteristics of the model to ensure that the model has converged to a solution (Ebert-Uphoff & Deng, 2012).

5.2 | Results and interpretation

5.2.1 | Jet speed and Arctic temperature

The VAR and LASSO models (Figure 2a,b) show both the magnitudes and the signs of the jet speed-Arctic temperature ($\mathcal{S}$-$\mathcal{T}$) relationship. For LASSO (Figure 2b), only the significant (nonzero) coefficients are shown, whereas all coefficients are shown for the VAR model (Figure 2a). Thus, lag days and coefficients that appear in both the LASSO and VAR models can be considered robust. To begin, we note that it is clear that the VAR and LASSO models are quite similar—the signs of the coefficients that appear in both models are largely the same, and their magnitudes are similar as well. The lags with the strongest coefficients are the same for both VAR and LASSO. For both the LASSO and the VAR models, both $\mathcal{S}$ and $\mathcal{T}$ are autocorrelated (curved arrows), with coefficients that decay over the 25-day period but remain nonzero. $\mathcal{T}$ drives $\mathcal{S}$ 5 days later (as well as 10, 15, and 20 days later), with the positive coefficient indicating that warmer temperatures drive a faster jet in the North Pacific. $\mathcal{S}$ also drives $\mathcal{T}$ at a lag of 5 days, with the negative coefficient indicating that faster jets are associated with a colder Arctic. However, at a lag of 15 days and beyond, the relationship between $\mathcal{S}$ and $\mathcal{T}$ changes—$\mathcal{S}$ drives $\mathcal{T}$ with positive LASSO coefficients, indicating that a stronger North Pacific jet drives warmer Arctic temperatures. Collectively, the LASSO results indicate that there is a positive feedback loop between Arctic temperature and North Pacific jet speed—a warmer Arctic temperature drives a stronger North Pacific jet, and the stronger jet drives further Arctic warming.

The jet speed-temperature PC model (Figure 2c) agrees quite well with the results of the LASSO and VAR models, although its formulation does not provide the magnitudes or signs of the relationships. The autocorrelation relationships (curved arrows) in the PC model are quite similar to those in the LASSO model. In the PC model, $\mathcal{T}$ drives $\mathcal{S}$ at a lag of 5 days only, and $\mathcal{S}$ drives $\mathcal{T}$ at lags of 15 and 20 days. These lags in the PC match well with the coefficients having a large magnitude in the LASSO models, highlighting that the different methods yield very similar (although not identical) results. The only exception is that, for a lag of 5 days, LASSO picks up a moderately strong negative connection from $\mathcal{S}$ to $\mathcal{T}$, whereas PC does not confirm that connection. Figure 4a summarizes these results—the colors of the arrows indicate the sign of the relationship (determined from VAR and LASSO), whereas the significant lag days are determined by including only lags that are significant in both the LASSO and PC models.

5.2.2 | Jet latitude and Arctic temperature

Jet latitude, $\mathcal{L}$, also shows evidence of a causal relationship with $\mathcal{T}$ in the VAR, LASSO, and PC models (Figure 3). The influence of $\mathcal{T}$ on $\mathcal{L}$ is not as strong as the influence of $\mathcal{T}$ on $\mathcal{S}$, with both PC (Figure 3c) and LASSO (Figure 3b) showing few lags with significant relationships. In both the LASSO and VAR (Figure 3a,b) models, the $\mathcal{T}$ driving $\mathcal{L}$ relationship is negative at a lag of 5 days and positive at a lag of 10 days. However, the PC model shows that the $\mathcal{T}$ driving $\mathcal{L}$ connection is only significant at 5 days; thus, we consider only the signs of the 5-day coefficients. This negative coefficient at a lag of 5 days indicates that warmer Arctic temperatures drive an equatorward shift of the jet in the North Pacific, consistent with results from previous modeling studies (Deser et al., 2010; Magnusdottir et al., 2004; Peings & Magnusdottir, 2014).

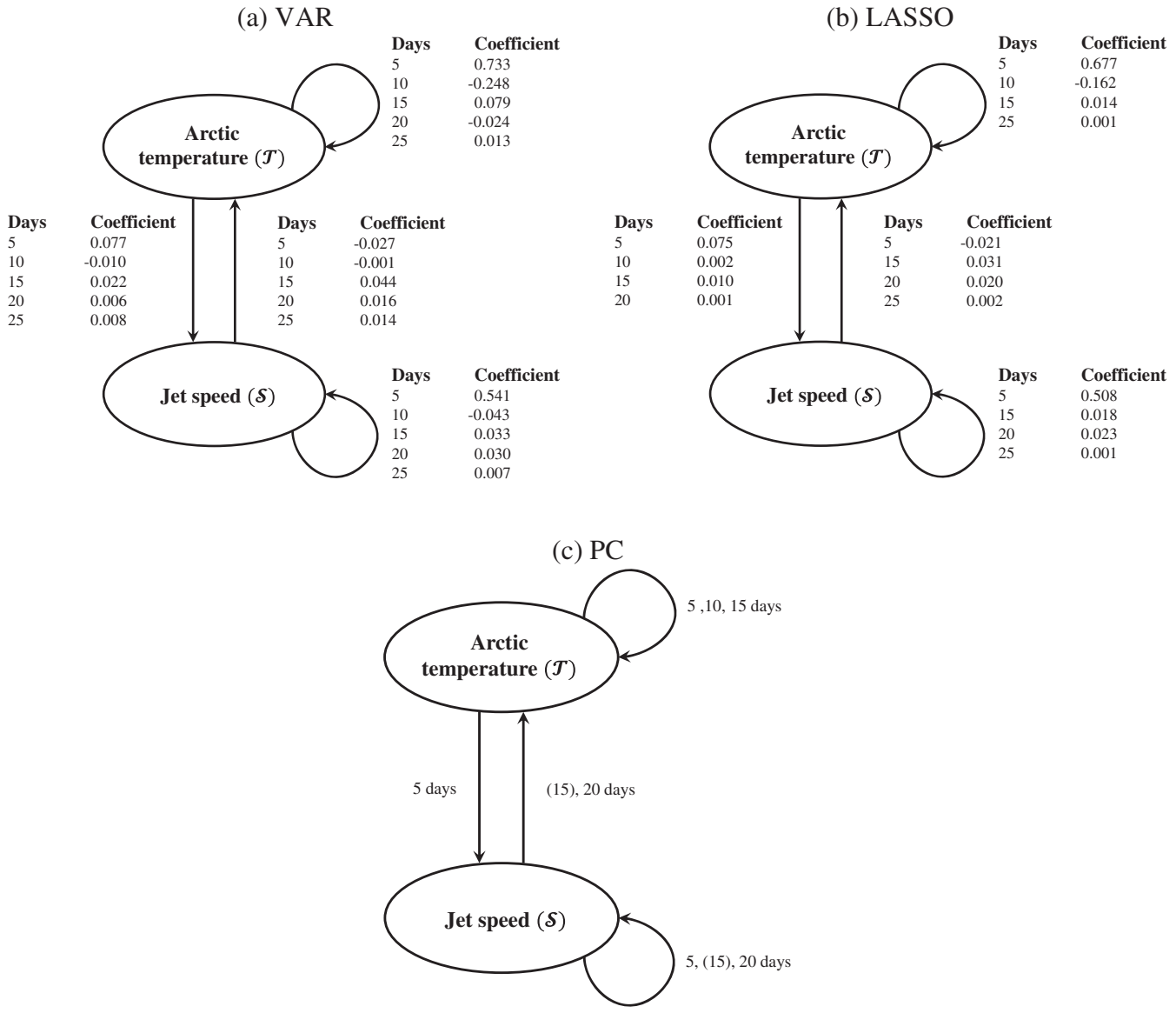

FIGURE 2 Arctic temperature ($\mathcal{T}$) and jet speed ($\mathcal{S}$) relationships as described by (a) VAR ($p = 5$), (b) LASSO ($\lambda = 0.0179, p = 5$), and (c) PC (11 time slices, $\alpha = 0.05$) models. Parentheses in PC results denote weak relationships. VAR = vector autoregression; LASSO = least absolute shrinkage and selection operator

While the $\mathcal{T}$ driving $\mathcal{L}$ relationship is relatively weak, the influence of $\mathcal{L}$ on $\mathcal{T}$ is stronger. The LASSO and VAR models show that $\mathcal{L}$ drives $\mathcal{T}$ with negative coefficients at most lags, indicating that a more equatorward jet drives warmer Arctic temperatures and a more poleward jet drives cooler Arctic temperatures. This relationship is strongest at a 5-day lag; it also strengthens at a 25-day lag in the VAR model. The PC model shows a very similar relationship to the LASSO model–$\mathcal{L}$ drives $\mathcal{T}$ at a lag of 5 days, with a resurgence at 20–25 days.

Like the positive feedback loop found between $\mathcal{T}$ and $\mathcal{S}$ (Figure 2), the positive feedback loop in Figure 3 indicates that the jet position-Arctic temperature feedback loop also acts to enhance Arctic warming. This positive feedback loop between jet position and Arctic temperature is more simply represented in Figure 4b. Dynamically, a more equatorward jet could act to enhance Arctic warming via increased cyclonic Rossby wave breaking activity on the poleward flank of the jet stream (Barnes & Hartmann, 2012), which increases moisture transport into the Arctic and, thus, atmospheric absorption of longwave radiation (Liu & Barnes, 2015; Woods et al., 2013), further warming the Arctic.

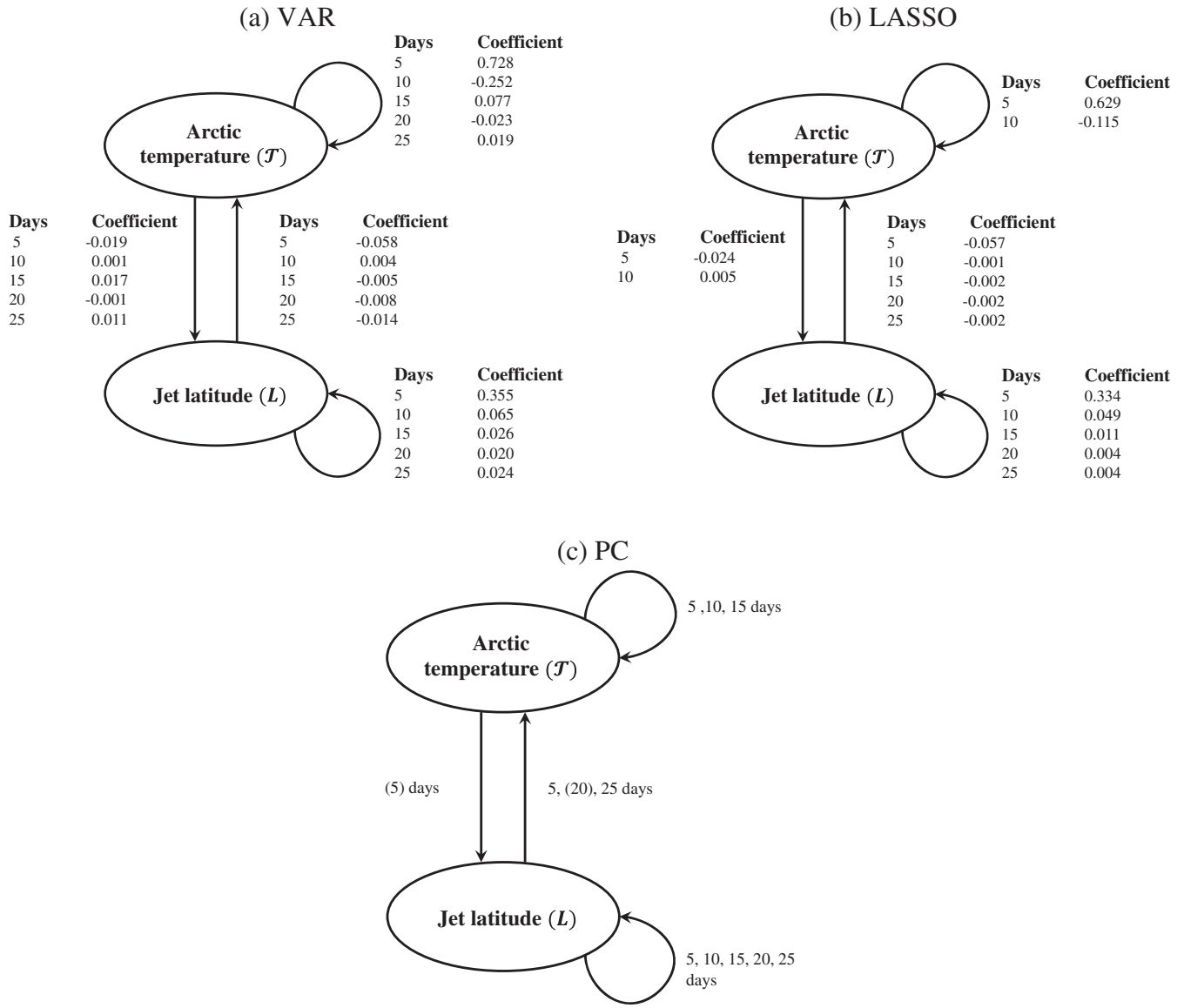

FIGURE 3 Arctic temperature ($\mathcal{T}$) and jet latitude ($\mathcal{L}$) relationships as described by (a) VAR ($p = 5$), (b) LASSO ($\lambda = 0.0337, p = 5$), and (c) PC (11 time slices, $\alpha = 0.05$) models. Parentheses in PC results denote weak relationships. VAR = vector autoregression; LASSO = least absolute shrinkage and selection operator

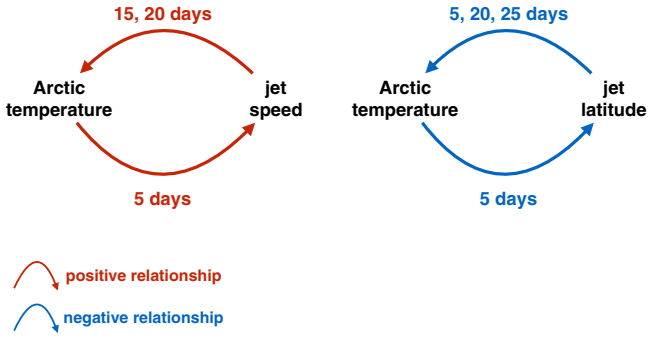

FIGURE 4 Minimalist graphs showing the dominant feedback loops and their time lags identified by all three methods when applicable. Note that the two positive relationships between arctic temperature and jet speed result in a positive (i.e., reinforcing) feedback loop. Similarly, the two negative relationships between arctic temperature and jet latitude together also result in a positive feedback loop

6 | DISCUSSION AND FUTURE WORK

Using VAR, LASSO, and PC models, we have quantified robust positive feedback loops between the North Pacific jet stream and Arctic temperatures on daily time scales. Specifically, a positive feedback loop is identified between jet speed and Arctic temperatures on time scales of 5–15 days, where a warmer Arctic drives a faster jet, and a faster jet drives a warmer Arctic. Similarly, a positive feedback loop is identified between jet latitude and Arctic temperatures, where a warmer Arctic drives a southward shift of the jet, which drives further Arctic warming.

Throughout this study, we mainly focused on the linear relationships between Arctic temperature and the jet stream variables. We used linear regression models to identify Granger causes while we used partial correlation-based (a measure of linear dependence) conditional independence tests in the PC algorithm to identify Pearl causes. However, the actual relationships in climate can be complex and nonlinear. By using nonlinear regression models (e.g., nonlinear random forests in Papagiannopoulou et al., 2017) along with statistical tests, one can identify nonlinear Granger dependencies between variables. It is possible that such nonlinear approaches would show higher sensitivity to Granger analysis, as they could pick up both the linear and nonlinear components of the causal relationship. In addition, the use of non-parametric conditional independence tests (for example, tests based on conditional mutual information) would allow one to capture linear and nonlinear Pearl dependencies from the PC algorithm without using any distributional assumptions for the data.

A limitation of any standard observational analysis, no matter whether based on Granger causality or Pearl causality, is the potential existence of hidden common causes. Results obtained from observation analysis must thus be interpreted with caution, that is, they should be interpreted as *hypotheses* that need to be confirmed by identifying the physical mechanisms behind each connection. The Fast Causal Inference (FCI) algorithm (Spirtes et al., 2000), which is an extension of the PC algorithm, can be helpful for alleviating this issue and is suggested to be studied in future work.

The work described here is only the beginning of a larger study that aims to apply causal discovery techniques to quantify Arctic-midlatitude connections. In future work, we plan to expand the current study to include (1) expansion of these methods to reanalysis, 2D spatial fields, and inclusion of additional variables such as sea ice extent; (2) results from significance testing by comparing unrestricted and restricted VAR models; (3) quantification of the strength of causal relationships with nonregression-based techniques. By applying causality techniques to the topic of Arctic-midlatitude connections, we aim not only to better understand the feedbacks between the Arctic and midlatitude weather but also to provide the climate science community with an example of how these powerful tools can offer new insights into complex earth science problems.

ACKNOWLEDGEMENTS

Support for this work was provided by National Science Foundation (NSF) grants AGS-1545675 (Barnes and McGraw) and AGS-1445978 (Ebert-Uphoff and Samarasinghe) under the CLD program.

ORCID

S. M. Samarasinghe https://orcid.org/0000-0002-1377-967X
M. C. McGraw https://orcid.org/0000-0002-4469-226X
E. A. Barnes http://orcid.org/0000-0003-4284-9320
I. Ebert-Uphoff http://orcid.org/0000-0001-6470-1947

REFERENCES

Bahadori, M. T., & Liu, Y. (2011). Granger causality analysis with hidden variables in climate science applications. Paper presented at Climate Informatics Workshop (CI 2011), Boulder, CO.

Barnes, E. A. (2013). Revisiting the evidence linking Arctic amplification to extreme weather in midlatitudes. *Geophysical Research Letters*, *40*, 4734–4739.

Barnes, E. A., Dunn-Sigouin, E., Masato, G., & Woollings, T. (2014). Exploring recent trends in Northern Hemisphere blocking. *Geophysical Research Letters*, *41*, 638–644.

Barnes, E. A., & Fiore, A. M. (2013). Surface ozone variability and the jet position: Implications for projecting future air quality. *Geophysical Research Letters*, *40*, 2839–2844.

Barnes, E. A., & Hartmann, D. L. (2012). Detection of Rossby wave breaking and its response to shifts of the midlatitude jet with climate change. *Journal of Geophysical Research: Atmospheres*, *117*.

Barnes, E. A., & Screen, J. A. (2015). The impact of Arctic warming on the midlatitude jet-stream: Can it? Has it? Will it? *WIREs Climate Change*, *6*, 277–286.

Butler, A. H., Thompson, D. W. J., & Heikes, R. (2010). The steady-state atmospheric circulation response to climate change-like thermal forcings in a simple general circulation model. *Journal of Climate*, *23*, 3474–3496.

Chen, X., Liu, Y., Liu, H., & Carbonell, J. G. (2010). Learning spatial-temporal varying graphs with applications to climate data analysis. *Proceedings of the Twenty-Fourth AAAI Conference on Artificial Intelligence*, Atlanta, GA.

Chu, T., Danks, D., & Glymour, C. (2005). *Data driven methods for nonlinear Granger causality: Climate teleconnection mechanisms* (Technical Report No. CMU-PHIL-171). Pittsburgh, PA: Department of Philosophy, Carnegie Mellon University.

Colombo, D., & Maathuis, M. H. (2014). Order-independent constraint-based causal structure learning. *The Journal of Machine Learning Research*, *15*(1), 3741–3782.

Deser, C., Tomas, R. A., Alexander, M., & Lawrence, D. (2010). The seasonal atmospheric response to projected Arctic sea ice loss in the late twenty-first century. *Journal of Climate*, *23*, 333–351.

Ebert-Uphoff, I., & Deng, Y. (2012). Causal discovery for climate research using graphical models. *Journal of Climate*, *25*(17), 5648–5665.

Ebert-Uphoff, I., & Deng, Y. (2015). Identifying physical interactions from climate data: Challenges and opportunities. *Computing in Science & Engineering*, *17*(6), 27–34.

Francis, J. A., & Vavrus, S. J. (2012). Evidence linking Arctic amplification to extreme weather in mid-latitudes. *Geophysical Research Letters*, *39*.

Gelaro, R., McCarty, W., Suárez, M. J., Todling, R., Molod, A., Takacs, L., … Zhao, B. (2017). The modern-era retrospective analysis for research and applications, version 2 (MERRA-2). *Journal of Climate*, *30*(14), 5419–5454.

Granger, C. W. J. (1969). Investigating causal relations by econometric models and cross-spectral methods. *Econometrica: Journal of the Econometric Society*, 424–438.

Granger, C. W. J. (1980). Testing for causality: A personal viewpoint. *Journal of Economic Dynamics and Control*, *2*(1), 329–352.

Hannart, A., Pearl, J., Otto, F. E. L., Naveau, P., & Ghil, M. (2016). Causal counterfactual theory for the attribution of weather and climate-related events. *Bulletin of the American Meteorological Society*, *97*(1), 99–110.

Hastie, T., Tibshirani, R., & Wainwright, M. (2015). *Statistical learning with sparsity: The lasso and generalizations*. Boca Raton, FL: Chapman and Hall/CRC.

Hoskins, B. J., & Hodges, K. I. (2002). New perspectives on the Northern Hemisphere, winter storm tracks. *Journal of the Atmospheric Sciences*, *59*, 1041–1061.

Ivanov, V., & Kilian, L. (2005). A practitioner's guide to lag order selection for VAR impulse response analysis. *Studies in Nonlinear Dynamics & Econometrics*, *9*(1).

Kay, J. E., Deser, C., Phillips, A., Mai, A., Hannay, C., Strand, G., … Vertenstein, M. (2015). The community earth system model (CESM) large ensemble project: A community resource for studying climate change in the presence of internal climate variability. *Bulletin of the American Meteorological Society*, *96*, 1333–1349.

Kretschmer, M., Coumou, D., Donges, J. F., & Runge, J. F. (2016). Using causal effect networks to analyze different arctic drivers of midlatitude winter circulation. *Journal of Climate*, *29*(11), 4069–4081.

Liu, C., & Barnes, E. A. (2015). Extreme moisture transport into the Arctic linked to Rossby wave breaking. *Journal of Geophysical Research: Atmospheres*, *120*, 3774–3788.

Liu, J., Curry, J. A., Wang, H., Song, M., & Horton, R. M. (2012). Impact of declining Arctic sea ice on winter snowfall. *Proceedings of the National Academy of Sciences of the United States of America*, *109*, 4074–4079.

Lund, R., Hurd, H., Bloomfield, P., & Smith, R. (1995). Climatological time series with periodic correlation. *Journal of Climate*, *8*, 2787–2809.

Lütkepohl, H. (2007). *New introduction to multiple time series analysis* (2nd ed.). Berlin, Germany: Springer-Verlag Berlin Heidelberg.

Magnusdottir, G., Deser, C., & Saravanan, R. (2004). The effects of North Atlantic SST and sea ice anomalies on the winter circulation in CCM3. Part I: Main features and storm track characteristics of the response. *Journal of Climate*, *17*, 857–876.

Matthewman, N. J., & Magnusdottir, G. (2011). Observed interaction between Pacific sea ice and the Western Pacific Pattern on intraseasonal time scales. *Journal of Climate*, *24*, 5031–5042.

McGraw, M. C., & Barnes, E. A. (2018). Memory matters: A case for Granger causality in climate variability studies. *Journal of Climate*, *31*, 3289–3300.

Melkumova, L. E., & Shatskikh, S. Y. (2017). Comparing ridge and LASSO estimators for data analysis. *Procedia Engineering*, *201*, 746–755.

Murphy, K. (2014). *Bayes net toolbox for Matlab (BNT)*. Available from https://github.com/bayesnet/bnt

Nicholson, W. B., Matteson, D. S., & Bien, J. (2017). VARX-L: Structured regularization for large vector autoregressions with exogenous variables. *International Journal of Forecasting*, *33*(3), 627–651.

Overland, J. E., & Wang, M. (2010). Large-scale atmospheric circulation changes are associated with the recent loss of Arctic sea ice. *Tellus*, *62*, 1–9.

Overpeck, J. T., Meehl, G. A., Bony, S., & Easterling, D. R. (2011). Climate data challenges in the 21st century. *Science*, *331*(6018), 700–702.

Papagiannopoulou, C., Miralles, D. G., Decubber, S., Demuzere, M., Verhoest, N. E. C., Dorigo, W. A., & Waegeman, W. (2017). A non-linear Granger-causality framework to investigate climate–vegetation dynamics. *Geoscientific Model Development*, *10*(1), 1945–1960.

Pearl, J. (1988). *Probabilistic reasoning in intelligent systems: Networks of plausible inference* (revised second printing). San Francisco, CA: Morgan Kaufman Publishers.

Pearl, J. (2000). *Causality: Models, reasoning and inference* (reprinted with corrections edition). Cambridge, UK: Cambridge University Press.

Peings, Y., & Magnusdottir, G. (2014). Response of the wintertime Northern Hemisphere atmospheric circulation to current and projected Arctic sea ice decline: A numerical study with CAM5. *Journal of Climate*, *27*, 244–264.

Pfaff, B. (2008). VAR, SVAR and SVEC models: Implementation within R package vars. *Journal of Statistical Software*, *27*(4), 1–32.

Qian, J., Hastie, T., Friedman, J., Tibshirani, R., & Simon, N. (2013). Glmnet for Matlab. Available from http://www.stanford.edu/~hastie/glmnet_matlab/

Rebane, G., & Pearl, J. (1987). The recovery of causal poly-trees from statistical data. *Proceedings of the Third Annual Conference on Uncertainty in Artificial Intelligence (UAI'87)*, Seattle, WA.

Runge, J. (2014). Detecting and quantifying causality from time series of complex systems (PhD thesis). Mathematisch-Naturwissenschaftliche Fakultät, Humboldt-Universität zu Berlin, Berlin, Germany.

Runge, J., Heitzig, J., Petoukhov, V., & Kurths, J. (2012). Escaping the curse of dimensionality in estimating multivariate transfer entropy. *Physical Review Letters*, *108*(25), 258701.

Samarasinghe, S., McGraw, M. C., Barnes, E. A., & Ebert-Uphoff, I. (2017). A study of causal links between the arctic and the midlatitude jet-streams. *Proceedings of the 7th International Workshop on Climate Informatics*, Boulder, CO. NCAR Technical Note NCAR/TN-536+PROC.

Screen, J. A., & Simmonds, I. (2010). The central role of diminishing sea ice in recent Arctic temperature amplification. *Nature*, *464*, 1334–1337.

Serreze, M. C., & Barry, R. G. (2005). *The arctic climate system*. Cambridge, UK: Cambridge University Press.

Spirtes, P., & Glymour, C. (1991). An algorithm for fast recovery of sparse causal graphs. *Social Science Computer Review*, *9*(1), 62–72.

Spirtes, P., Glymour, C., & Scheines, R. (2000). *Causation, prediction, and search* (2nd ed.). Cambridge, MA: MIT Press.

Strong, C., Magnusdottir, G., & Stern, H. (2009). Observed feedback between winter sea ice and the North Atlantic Oscillation. *Journal of Climate*, *22*(22), 6021–6032.

Tang, Q., Zhang, X., Yang, X., & Francis, J. A. (2013). Cold winter extremes in northern continents linked to Arctic sea ice loss. *Environmental Research Letters*, *8*.

Thomas, J. L., Waugh, D. W., & Gnanadesikan, A. (2015). Southern Hemisphere extratropical circulation: Recent trends and natural variability. *Geophysical Research Letters*, *42*, 5508–5515.

Tibshirani, R. (1996). Regression shrinkage and selection via the lasso. *Journal of the Royal Statistical Society Series B (Methodological)*, 267–288.

Wallace, J. M., & Gutzler, D. S. (1981). Teleconnections in the geopotential height field during the Northern Hemisphere winter. *Monthly Weather Review*, *109*, 784–812.

Wang, H., Banerjee, A., Hsieh, C.-J., Ravikumar, P. K., & Dhillon, I. S. (2013). *Large scale distributed sparse precision estimation*. Advances in Neural Information Processing Systems, 584–592.

Wettstein, J. J., & Wallace, J. M. (2010). Observed patterns of month-to-month storm-track variability and their relationship to the background flow. *Journal of the Atmospheric Sciences*, *67*, 1420–1437.

Woods, C., Caballero, R., & Svensson, G. (2013). Large-scale circulation associated with moisture intrusions into the Arctic during winter. *Geophysical Research Letters*, *40*, 4717–4721.

Woollings, T., Barnes, E., Hoskins, B., Kwon, Y.-O., Lee, R. W., Li, C., … Williams, K. (2018). Daily to decadal modulation of jet variability. *Journal of Climate*, *31*(4), 1297–1314.

Woollings, T., Hannachi, A., & Hoskins, B. (2010). Variability of the North Atlantic eddy-driven jet stream. *Quarterly Journal of the Royal Meteorological Society*, *136*, 856–868.

Zerenner, T., Friederichs, P., Lehnertz, K., & Hense, A. (2014). A Gaussian graphical model approach to climate networks. *Chaos: An Interdisciplinary Journal of Nonlinear Science*, *24*(2), 023103.

SUPPORTING INFORMATION

Additional supporting information may be found online in the Supporting Information section at the end of the article.

How to cite this article: Samarasinghe SM, McGraw MC, Barnes EA, Ebert-Uphoff I. A study of links between the Arctic and the midlatitude jet stream using Granger and Pearl causality. *Environmetrics*. 2019;30:e2540. https://doi.org/10.1002/env.2540

APPENDIX

DETAILS OF THE GROUP LASSO APPROACH

In general, a standard LASSO approach is adequate to perform a basic Granger analysis. In contrast to the standard LASSO approach, the *group* LASSO approach (Hastie et al., 2015; Nicholson et al., 2017) is often useful if the predictors show a natural group structure, as is the case for time series data. By treating a group of coefficients as a collective entity and

constraining that group (rather than the individual coefficients), this approach forces entire groups of coefficients to be zero, rather than individual coefficients. In our case, the groups are based on the predictor variables (where predictor variables $= \{\{z_{m,t-i}\}_{t=p+1}^{T} | i = 1, \ldots, p \text{ and } m = 1, \ldots, k\}$) and the coefficients of any particular predictor variable are all set to zero if that predictor does not contribute to the predictability of *any* of the response variables. The specific version used here solves the optimization problem given in Equation (A1), where $a^{i}_{.,m}$ denotes the mth column in $\mathbf{A_i}$ and $N = (T - p)$ is the effective sample size.

$$\min_{\mathbf{A,c}} \quad \frac{1}{2N} \sum_{t=p+1}^{T} \|\mathbf{z_t} - \mathbf{c} - \sum_{i=1}^{p} \mathbf{A_i z_{t-i}}\|_2^2 + \lambda \sum_{i=1}^{p} \sum_{m=1}^{k} \|a^{i}_{.,m}\|_2 \quad \lambda \geq 0 \tag{A1}$$

Finally, the literature suggests that the elastic net, which is a regularization technique incorporating both l_1 and l_2 constraints, can be more useful than LASSO when predictors are highly correlated, which is often the case with many climate variables (Hastie et al., 2015). However, in our study, the use of an elastic net did not provide any noteworthy changes in the dependency structure compared to the LASSO results.